

Fracture Mechanisms in Multilayer Phosphorene Assemblies: From Brittle to Ductile

Ning Liu¹, Jiawang Hong², Xiaowei Zeng³, Ramana Pidaparti^{1*} and Xianqiao Wang^{1*}

¹College of Engineering, University of Georgia, Athens, GA 30602 USA

²Department of Applied Mechanics, Beijing Institute of Technology, Beijing 100081, China

³Department of Mechanical Engineering, University of Texas at San Antonio, San Antonio, TX 78249
USA

*Corresponding author: xqwang@uga.edu and rmparti@uga.edu

1. Dependence of ultimate strength σ_u and plateau stress σ_p on flake number n_f

Actually, in order to obtain the relationship between the thickness and ultimate strength σ_u , three assumptions should be made. First, the energy barrier per area γ required to overcome the initiation of the interfacial sliding is a material constant. Secondly, the axial stress along the loading direction is uniform as long as the overlap distance L_{ol} is sufficiently long. Finally, prior to the nucleation of the interlayer sliding MLPs behave like a linear elastic material. When the overlap distance is not sufficiently long, typically smaller than twice of the effective interaction length l_e , the conclusion in Figure 7 does not hold any more. Therefore, a series of simulations are performed when the overlap distance L_{ol} is fixed at 8.94 nm and the flake number varies from 1 to 6. Corresponding stress-strain responses are shown in Figure S7(a). It can be seen that when the flake number is equal to 1, the sample experiences brittle failure as expected. As the flake number increases, the fracture pattern shifts from brittle to ductile. The ultimate strength σ_u are captured and shown in Figure S7(b). Results indicate that for the fitting curve, both the constant α (5.576) and the exponent coefficient (-0.806) are different from those in Figure 7(a). With respect to plateau stress σ_p , the fitted curves are also different from those in Figure 7(b) as shown in Figure S7(c).

In order to verify the results in Figure 7, additional simulations have been carried out when the overlap distance is 52.03 nm. Corresponding stress-strain responses are shown in Figure S8(a). Besides, the results about the ultimate strength σ_u are collected and shown in Figure S8(b). It can be seen that both the constant α (4.54) and the exponent (-0.5) are very close to those in Figure 7(a) (4.64 and -0.5, respectively). Regarding plateau stress σ_p , the constant α (4.40) and the exponent (-0.62) as shown in Figure S8(c) are also very close to those in Figure 7(b) (4.61 and -2/3).

In summary, the model is only appropriate for the plateau values.

2. Calculation of Interlayer Adhesion γ_{ad}

The interlayer adhesion is of critical importance to the strength and toughness of the system. In this revised manuscript, two strategies are employed in order to calculate the adhesion γ_{ad} and the corresponding results are shown in Figure S10 and S11. The first strategy is to separate two

adjacent phosphorene flake in the out-of-plane (thickness) direction. The corresponding geometrical parameters have been marked in Figure S10 (a). Periodic boundary conditions are adopted along the x and y direction while free boundary condition is adopted along the z direction. The initial inter-flake distance is 5.54 Å. First, energy minimization is performed to get the initial potential energy of the system. Subsequently, the upper flake is moved 10 Å each time and energy minimization is performed again to get the potential energy until the displacement reaches to 30 Å. Therefore, the potential energy difference between the final and initial state is considered as the work done to separate two flakes, which is divided by the area to get the interlayer adhesion. The final value for γ_{ad} is 0.345 J/m².

In addition to separation, a pseudo pulling-out test is also adopted to calculate the interlayer adhesion γ_{ad} . The corresponding geometrical parameters are shown in Figure S11(a). Four flakes are included in this system, periodic boundary conditions are adopted in the y and z directions, and free boundary condition is adopted in the x direction. The initial inter-flake distance is 5.54 Å. First, energy minimization is performed to get the initial potential energy. Subsequently, the two flakes in the middle are displaced a lattice constant along the x direction (zigzag direction), 3.31Å, each time and energy minimization is performed again to get the potential energy until the displacement reaches to 33.1 Å. Due to the incompleteness of the edges, the energy difference between the first step and the initial state is smaller. Thus, the first step is ignored. The energy different between the final stage and the first displacement is calculated and considered as the work done to create new surfaces, which is divided by the area of the new surface to calculate the adhesion γ_{ad} . The final value is 0.342 J/m², which is very close to the previous result.

3. Relationship between residual overlap distance l_r and effective interaction length l_e

The residual overlap distance l_r measured as shown in Figure 8(c) and listed in Table S2. For comparison purpose, the effective interaction length l_e is also listed in Table S2. As we can see, the residual overlap distance l_r is roughly twice of the effective overlap distance. For each flake number n_f , only one case has been run, which is a slight modeling limitation. Note that since the fracture of MLPs is a random process, multiple simulations with different initial velocity profile should be performed for each flake number n_f in order to better capture the ratio between the residual overlap distance l_r and effective overlap distance l_e .

Figure

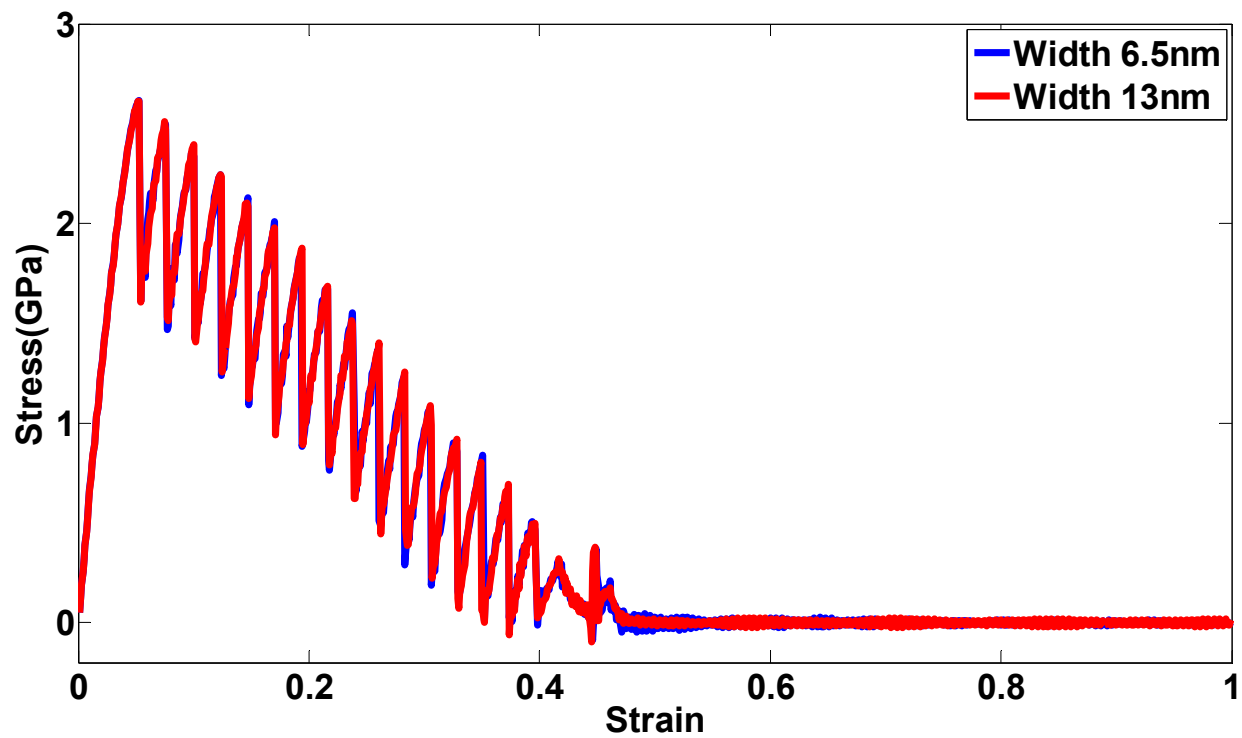


Figure S1. Stress-strain responses under uniaxial tensile test along the zigzag direction for samples with different widths (The overlap distance L_{ol} is equal to 5.63nm; The number of phosphorene flakes per layer n_f is fixed at 2).

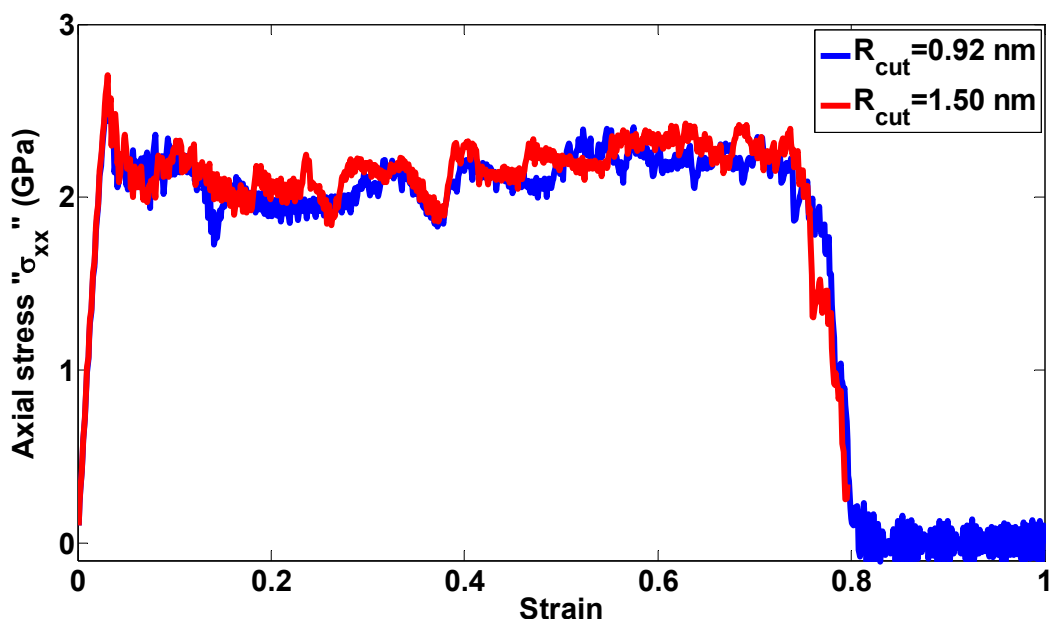


Figure S2. The effect of different cutoff radius for Lennard-Jones potential on stress-strain responses under uniaxial tensile tests along the zigzag direction (When the overlap distance L_{ol} is equal to 38.77 nm; The number of flakes per layer n_f is fixed at 3).

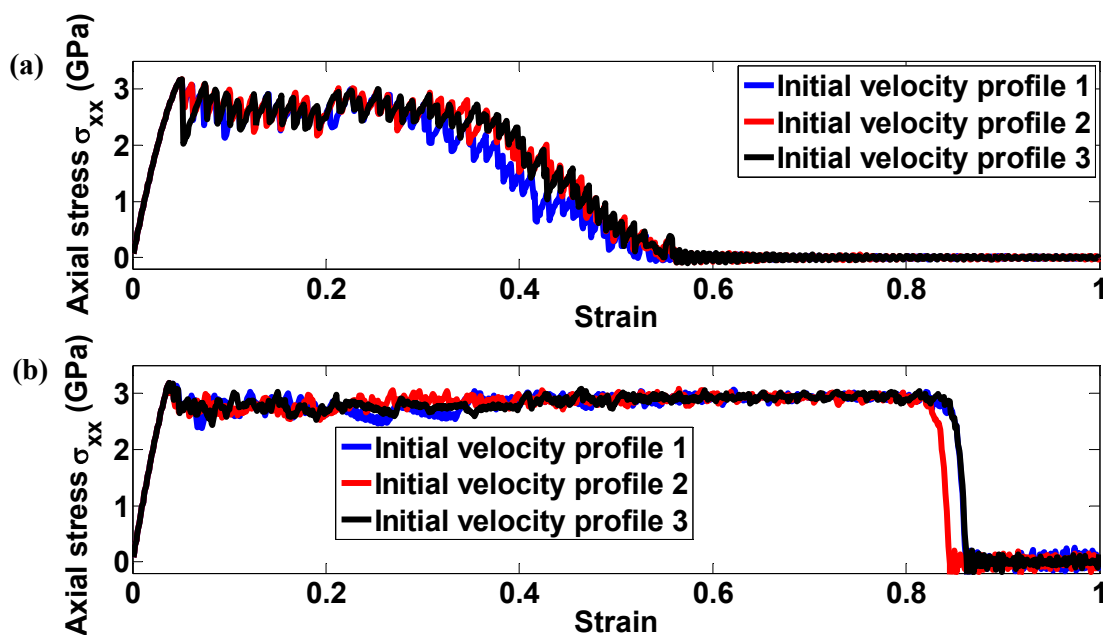


Figure S3. Stress-strain responses under uniaxial tensile test along the zigzag direction when the initial velocity profile is different (a) Overlap distance $L_{ol} = 12.26$ nm; (b) Overlap distance $L_{ol} = 38.77$ nm (The number of phosphorene flakes per layer n_f is fixed at 2).

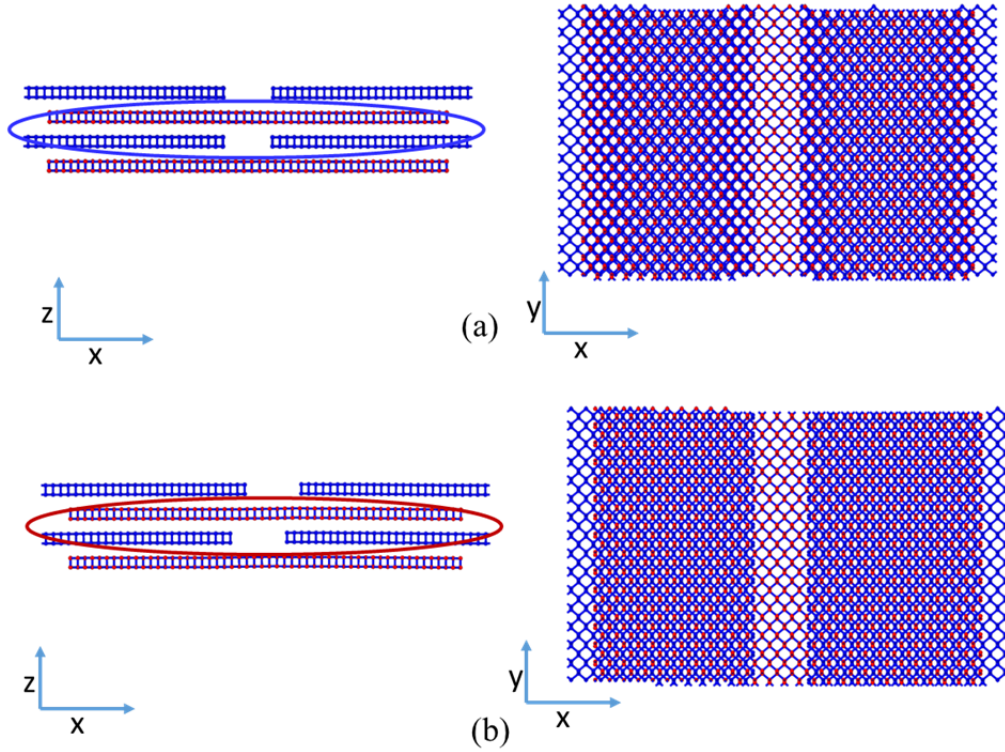


Figure S4. Geometrical configurations (a) before the nucleation of slip pulse; (b) after the nucleation of slip pulse when the overlap distance L_{ol} and the flake number n_f are 3.97nm and 1, respectively. (Note that front views from the y direction are shown on the left side and top views from z direction of the two selected flakes in the middle are shown on the right side.)

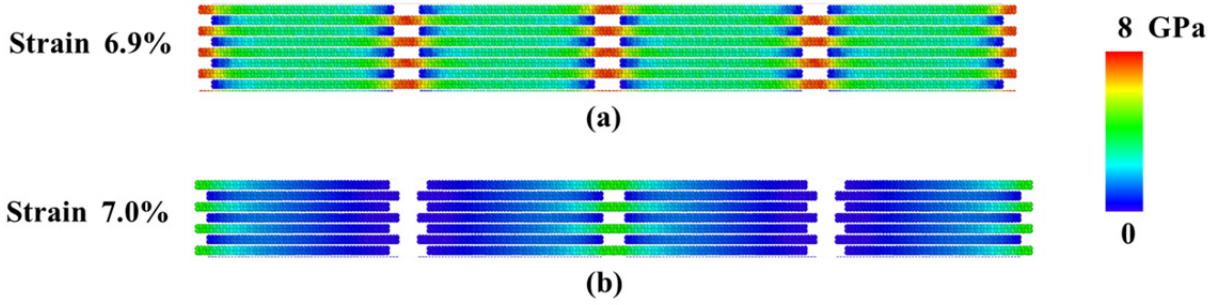


Figure S5 Axial Stress profile (a) before and (b) after rupture ($L_{ol} = 8.94$ nm).

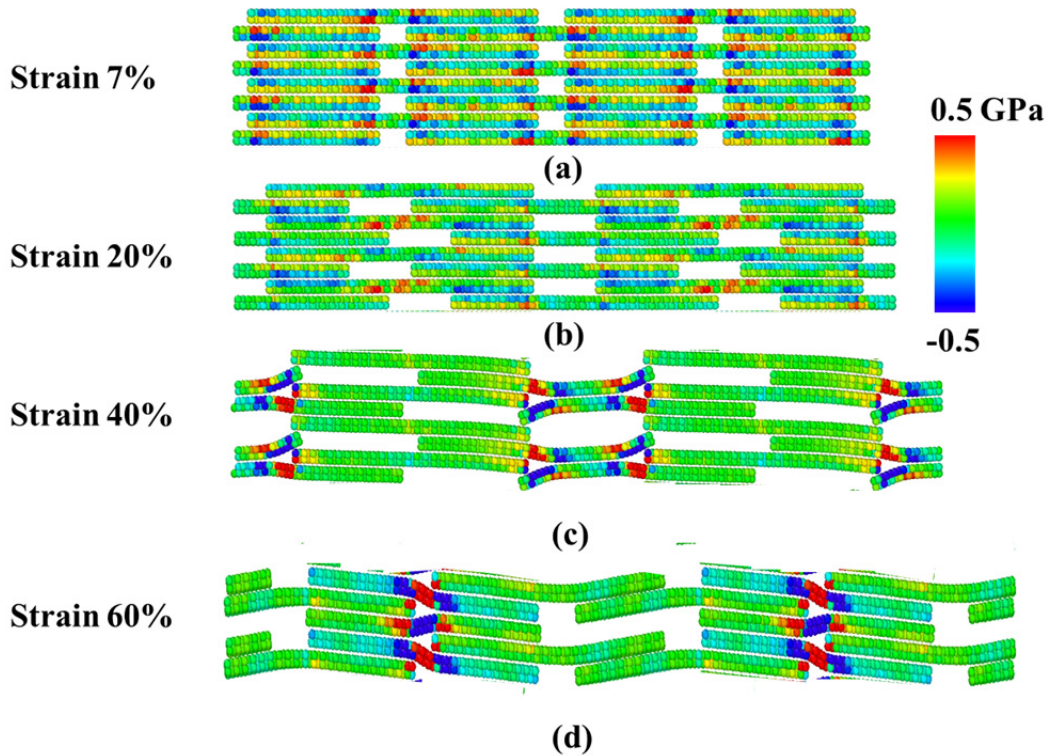


Figure S6 Shear stress profile during the tensile test when overlap distance L_{ol} is 3.97 nm (a) right before the nucleation of the first interfacial sliding; (b) during the first interfacial sliding; (c) close to the end of the first sliding; (d) during the second interfacial sliding (colored by axial stress; $n_f = 1$; for visualization purpose, the sample is reproduced two times along thickness and loading direction; the sequence numbers are related to the insets in Figure 2).

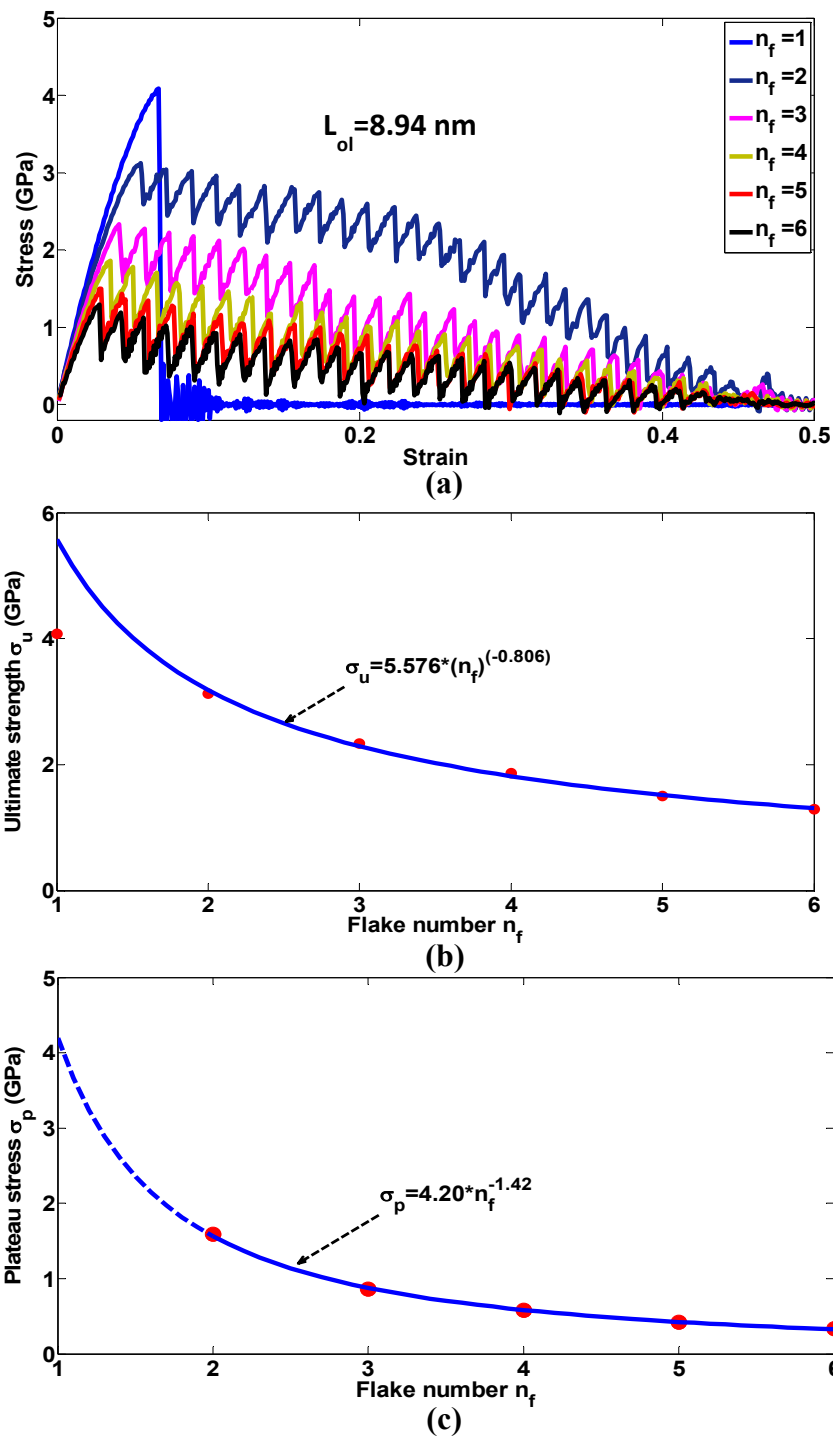


Figure S7 Tensile tests for MLPs with different flake number n_f ($L_{ol} = 8.94$ nm) (a) stress-strain responses (b) ultimate strength versus flake number n_f . (red dots represent results from simulations and the blue curve represents the results through curve fitting).

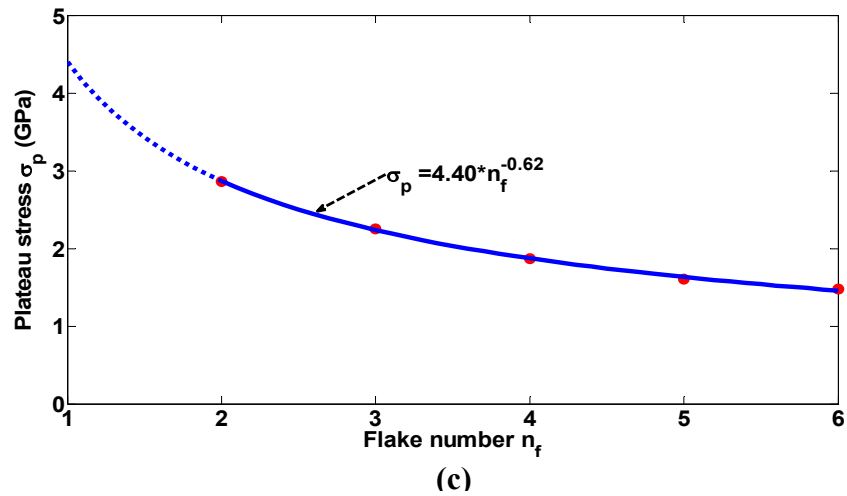
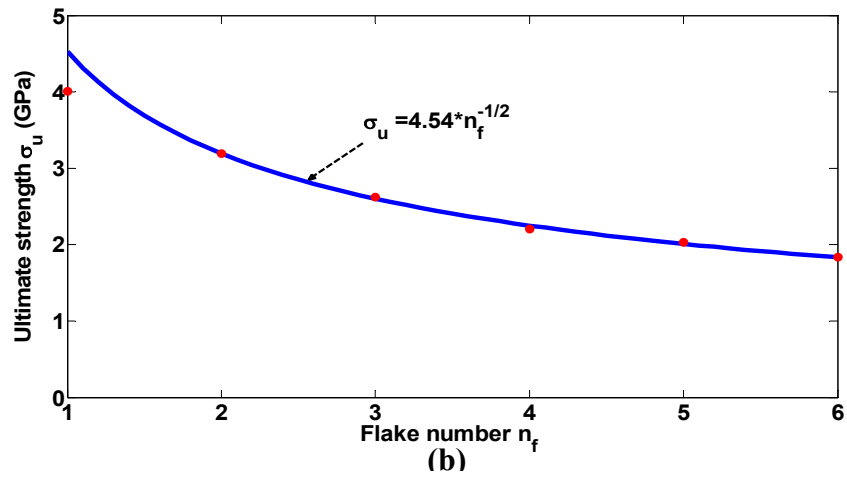
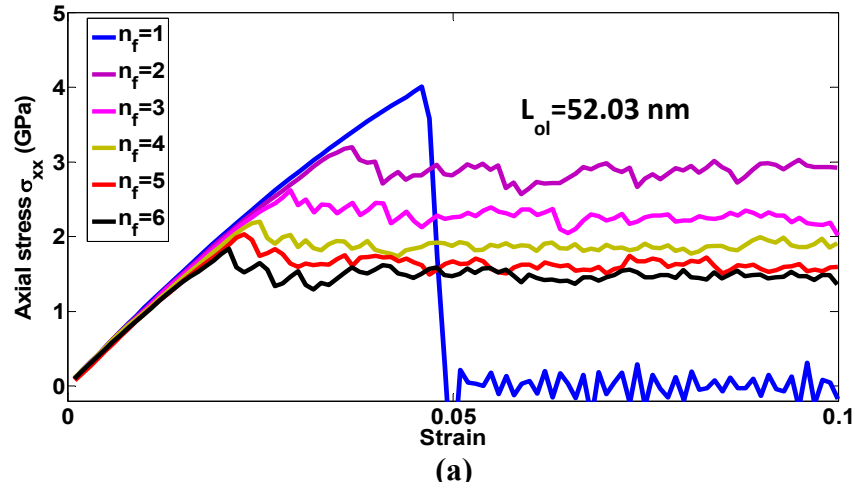


Figure S8 Tensile tests for MLPs with different flake number n_f ($L_{ol} = 52.03\text{nm}$) (a) stress-strain responses (b) ultimate strength versus flake number n_f . (red dots represent results from simulations and the blue curve represents the results through curve fitting).

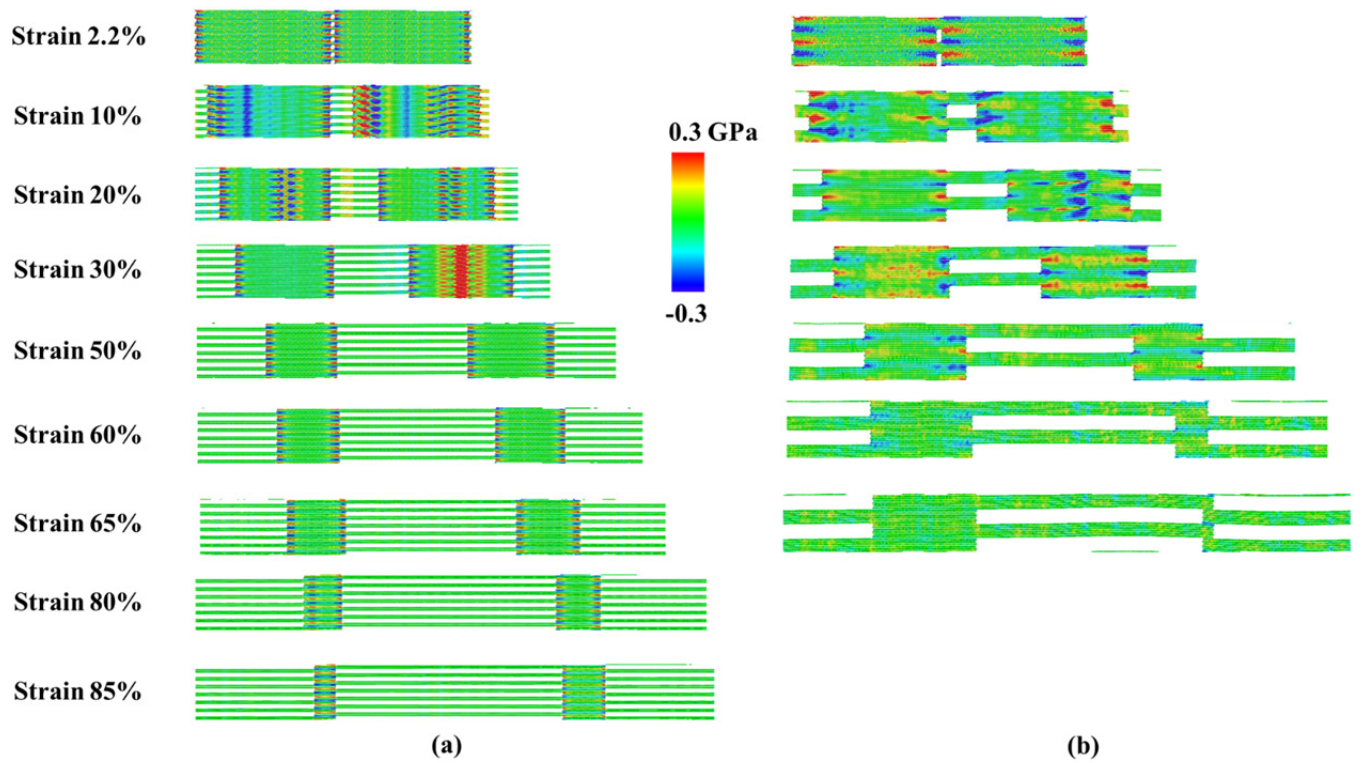


Figure S9 Relative strain map of the tensile dynamics of (a) samples with 2 flakes per layer ($n_f = 2$); (b) samples with 6 flakes per layer ($n_f = 6$). (For visualization purpose, the samples are reproduced 2 and 6 times for $n_f = 2$ and $n_f = 6$ respectively along the thickness direction; The snapshots are false colored by shear stress along the loading direction).

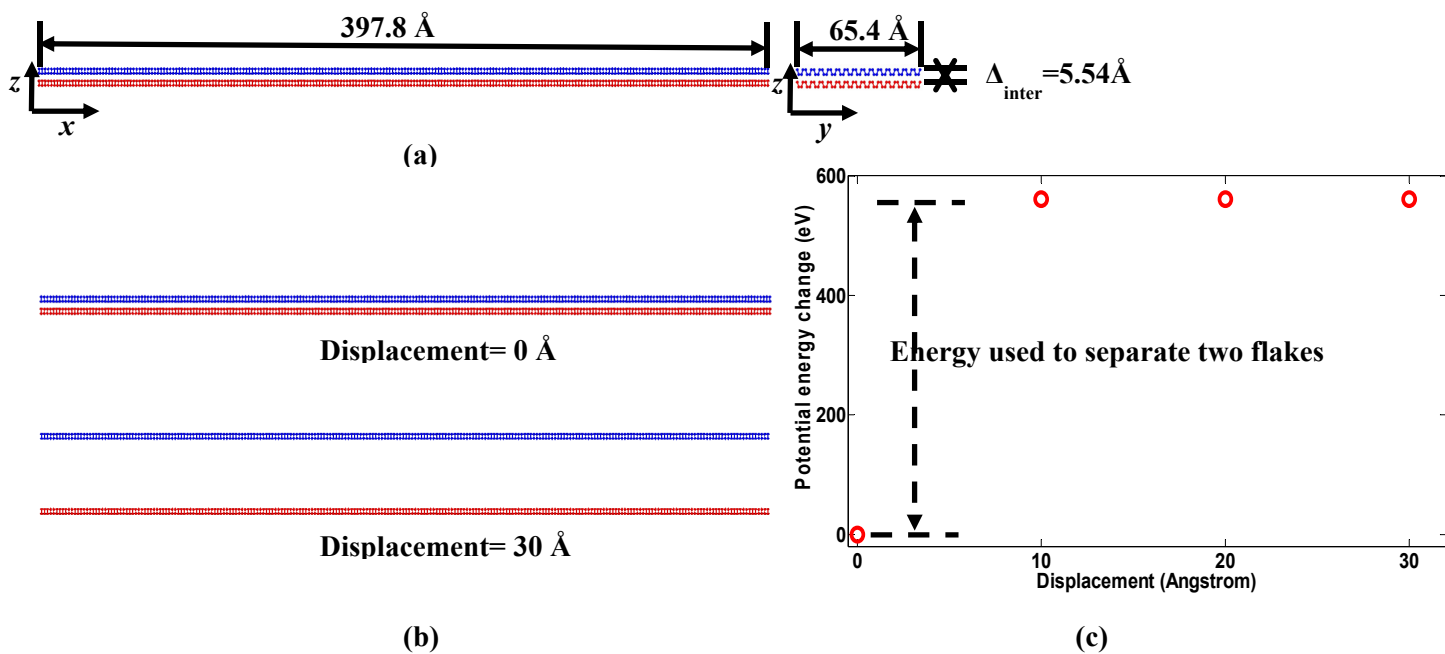


Figure S10 Adhesion calculation through separation.

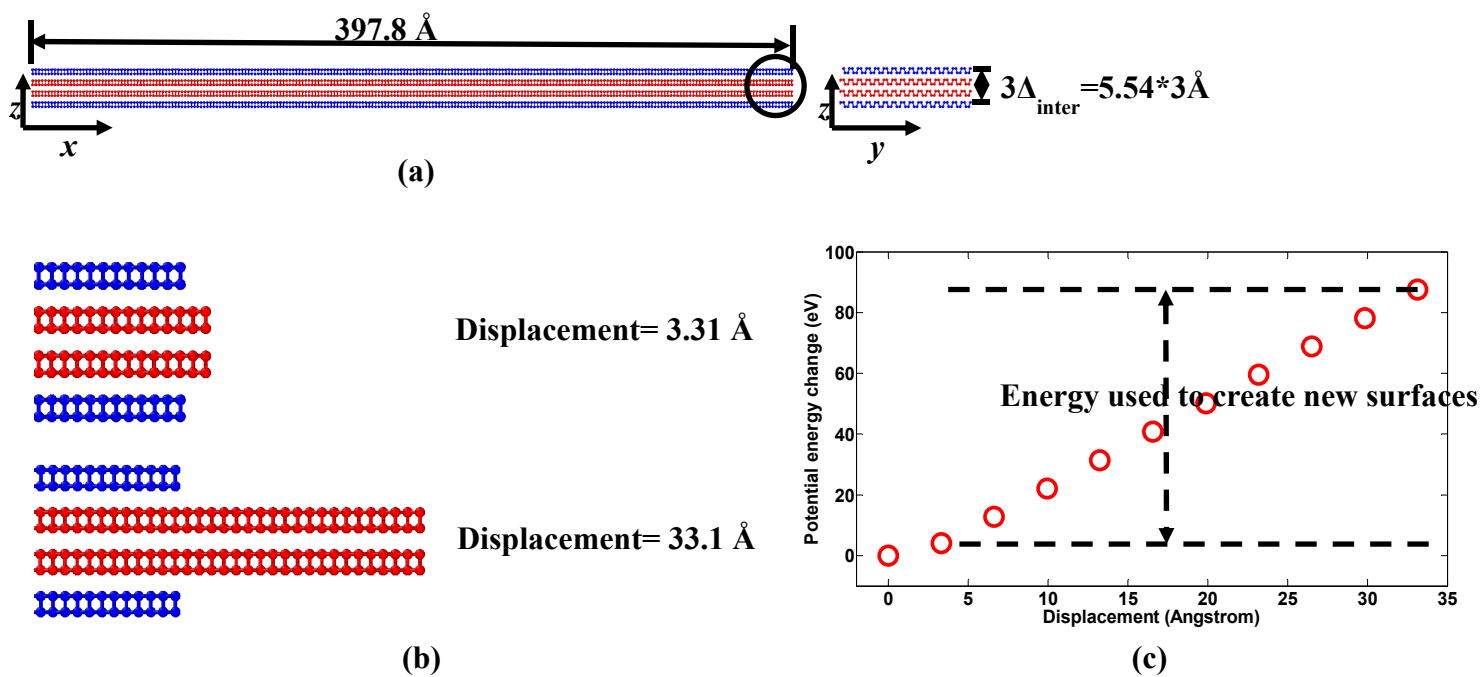


Figure S11 Adhesion calculation through pull-out.

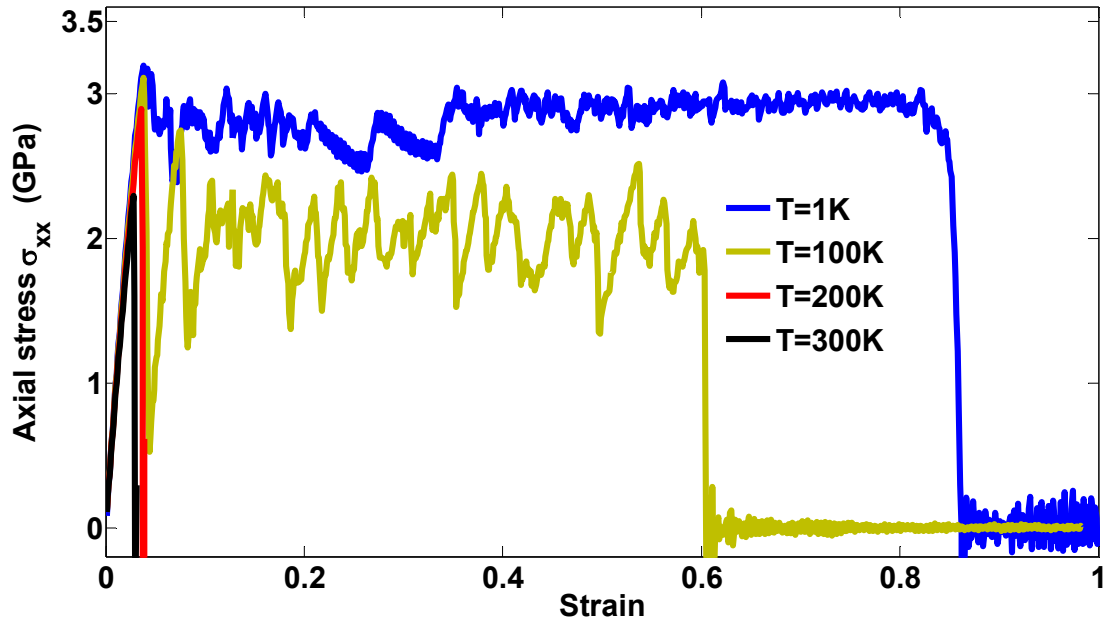


Figure S12 Stress-strain responses of MLPs ($n_f = 2, L_{ol} = 38.7 \text{ nm}$) at different temperatures.

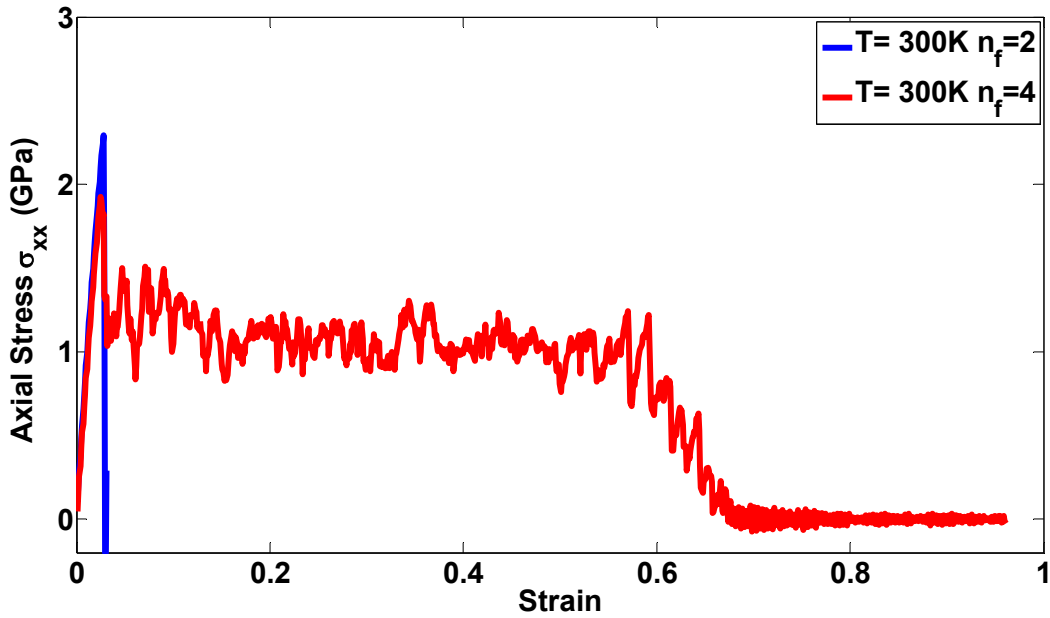


Figure S13 Stress-strain responses of MLPs with different flake number n_f ($L_{ol} = 38.7 \text{ nm}$) at room temperature.

Tables

Table S1. Parameters of the SW potential. “tol” represent a controllable parameter of the SW potential form in LAMMPS. Pt represents atoms located on the top region while Pb represents atoms from the bottom region.

	$\epsilon(\text{eV})$	$\sigma(\text{\AA})$	a	λ	γ	$\cos\theta_0$	A	B	p	q	tol
Pt-Pt-Pt	1.000	0.809	3.449	35.701	1.000	-0.111	3.626	33.371	4	0	0.0
Pb-Pb-Pb	1.000	0.809	3.449	35.701	1.000	-0.111	3.626	33.371	4	0	0.0
Pt-Pt-Pb	1.000	0.809	3.449	32.006	1.000	-0.210	0.000	33.371	4	0	0.0
Pb-Pb-Pt	1.000	0.809	3.449	32.006	1.000	-0.210	0.000	33.371	4	0	0.0

Table S2. The comparison of effective interaction length l_e and residual overlap distance l_r

	$n_f = 2$	$n_f = 3$	$n_f = 4$	$n_f = 5$	$n_f = 6$
Effective interaction length $l_e(\text{nm})$	5.0	6.3	8.1	9.1	10.3
Residual overlap distance $l_r(\text{nm})$	11.9	13.9	13.8	19.2	23.8

Table S3. The comparison of ultimate strength between the MLPs ($L_{ol}=38.7\text{nm}$ $n_f=2$) and single-flake phosphorene at different environmental temperature (Blue represents cases that interlayer sliding happens and Red represents cases that no interlayer sliding happens.)

	T=1K	T=100K	T=200K	T=300K
Single-flake phosphorene²	7.96 GPa	6.04 GPa	4.92GPa	3.82 GPa
MLPs ($n_f=2$ $L_{ol}=38.7\text{nm}$)	3.14 GPa	3.10 GPa	2.89GPa	2.29GPa